LETTER

doi:10.1038/nature11808

Biguanides suppress hepatic glucagon signalling by decreasing production of cyclic AMP

Russell A. Miller[1], Qingwei Chu[1], Jianxin Xie[2], Marc Foretz[3,4,5], Benoit Viollet[3,4,5] & Morris J. Birnbaum[1]

Glucose production by the liver is essential for providing a substrate for the brain during fasting. The inability of insulin to suppress hepatic glucose output is a major aetiological factor in the hyperglycaemia of type-2 diabetes mellitus and other diseases of insulin resistance[1,2]. For fifty years, one of the few classes of therapeutics effective in reducing glucose production has been the biguanides, which include phenformin and metformin, the latter the most frequently prescribed drug for type-2 diabetes[3]. Nonetheless, the mechanism of action of biguanides remains imperfectly understood. The suggestion a decade ago that metformin reduces glucose synthesis through activation of the enzyme AMP-activated protein kinase (AMPK) has recently been challenged by genetic loss-of-function experiments[4]. Here we provide a novel mechanism by which metformin antagonizes the action of glucagon, thus reducing fasting glucose levels. In mouse hepatocytes, metformin leads to the accumulation of AMP and related nucleotides, which inhibit adenylate cyclase, reduce levels of cyclic AMP and protein kinase A (PKA) activity, abrogate phosphorylation of critical protein targets of PKA, and block glucagon-dependent glucose output from hepatocytes. These data support a mechanism of action for metformin involving antagonism of glucagon, and suggest an approach for the development of antidiabetic drugs.

Biguanides exert their major effect through inhibition of liver glucose production, although enhanced glucose disposal has also been noted in some studies[5,6]. Despite the wide acceptance of metformin as a first-line therapeutic for diabetes, its mechanism of action remains unclear. Metformin inhibits mitochondrial respiratory complex 1, thus reducing hepatic energy charge; ten years ago it was suggested that metformin functioned through activation of the kinase AMPK[7–10]. This has been challenged recently in experiments using livers and primary hepatocytes lacking either AMPK or its upstream activating enzyme LKB1 (ref. 4). Because both glycogenolysis and gluconeogenesis are controlled during the fasting state in part by the hormone glucagon, the abnormal secretion of which is a major factor in the pathophysiology of hyperglycaemia in type-2 diabetes, we explored the idea that metformin produces its effects by inhibiting glucagon signalling pathways[11–13].

Binding of glucagon to its receptor on the hepatocyte plasma membrane leads to activation of adenylyl cyclase, production of the second-messenger cyclic AMP (cAMP) and stimulation of PKA, which phosphorylates protein targets that work in concert to increase hepatic glucose output[12]. In primary mouse hepatocytes, we tested a panel of compounds that activate AMPK by decreasing energy charge or mimicking a reduced energy charge for the inhibition of glucagon-dependent increases in cAMP. Treatment with all agents increased AMPK phosphorylation and antagonized the glucagon-dependent elevation in cAMP (Supplementary Fig. 1a, b). Phenformin showed a dose-dependent inhibition of glucagon-induced cAMP accumulation with a half-maximal inhibitory concentration of ~150 μM, which correlated well with its effect on intracellular AMP (Fig. 1a, b). To mimic more closely the chronic treatment of diabetic patients with biguanides, we tested 24-h exposure of hepatocytes to phenformin or metformin for a reduction in glucagon-increased cAMP levels. After long-term treatment, phenformin was effective at considerably lower concentrations, with concentrations of 10 μM or greater causing significant reductions in glucagon-stimulated increases in cAMP levels (Fig. 1c). Metformin also inhibited cAMP accumulation at concentrations of 125 μM or greater, levels slightly higher than in the serum of diabetic patients after taking a 1 mg dose of metformin but probably similar to those accumulated in splanchnic tissues[14,15] (Fig. 1d). In rats, administration of a therapeutic dose of 50 mg kg^{-1} leads to levels greater than 250 μM in the liver [14,15]. Like phenformin, therapeutic concentrations of metformin elicited significant increases in AMP levels in primary hepatocytes (Supplementary Fig. 2a–c). Glucagon did not alter adenine nucleotide levels or activate AMPK in primary hepatocytes and did not affect the changes produced by metformin (Supplementary Fig. 2a–d).

To determine the effects of phenformin on the kinetics of activation of PKA, we used the AKAR3 fluorescence resonance energy transfer (FRET) reporter[16]. Primary hepatocytes were infected with adenovirus encoding AKAR3 and 18 h later confocal images were acquired over time (Supplementary Fig. 3a). Glucagon increased the FRET ratio (FRET/cyan fluorescent protein (CFP)) of AKAR3 in the cytoplasm of hepatocytes within 1 min and reached a maximum at 2 min, thereafter exhibiting only minimal decay for 15 min. Phenformin both delayed the rise in PKA activity and accelerated its decay (Supplementary Fig. 3b). The concentration dependence of inhibition of PKA activity measured biochemically was similar to blockade of cAMP accumulation in primary hepatocytes (Fig. 1e). AICAR, an adenosine analogue that can be phosphorylated to form the AMP mimetic ZMP, also antagonized the glucagon-dependent increase of PKA activity in isolated hepatocytes (Supplementary Fig. 4a).

Treatment of primary hepatocytes with phenformin inhibited the glucagon-dependent phosphorylation of cellular proteins at PKA substrate motifs (Fig. 1f). Phenformin also antagonized phosphorylation of the PKA substrates PFKFB1 and the inositol-1,4,5-trisphosphate receptor IP3R (also known as ITPR1), as revealed by western blots using phospho-specific antibodies against these proteins (Fig. 1f and Supplementary Fig. 5a). If reductions in levels of endogenous cAMP are important for the actions of biguanides, we would expect the latter to block PKA target phosphorylation in response to glucagon but not a membrane-permeable analogue of cAMP, SP-8Br-cAMPS-AM. Glucagon induced phosphorylation of the PKA target proteins PFKFB1, CREB (also known as CREB1) and IP3R in primary hepatocytes; phenformin activated AMPK and inhibited phosphorylation of these PKA target proteins (Fig. 2a and Supplementary Fig. 6a). In contrast, when SP-8Br-cAMPS-AM concentrations were used that elicited comparable phosphorylation of the PKA substrates, the actions of SP-8Br-cAMPS-AM were not antagonized by phenformin (Fig. 2b and Supplementary Fig. 6b). These results demonstrate that phenformin inhibits the glucagon- but not SP-8Br-cAMPS-AM-dependent phosphorylation of PKA substrates, a result most consistent with biguanides working at a signalling step upstream from the activation

[1]Institute for Diabetes, Obesity, and Metabolism, Perelman School of Medicine, University of Pennsylvania, Philadelphia, Pennsylvania 19104, USA. [2]Cell Signaling Technology, Inc., 3 Trask Lane, Danvers, Massachusetts 01923, USA. [3]Inserm, U1016, Institut Cochin, Paris 75014, France. [4]Cnrs, UMR8104, Paris 75014, France. [5]Université Paris Descartes, Sorbonne Paris cité, Paris 75006, France.

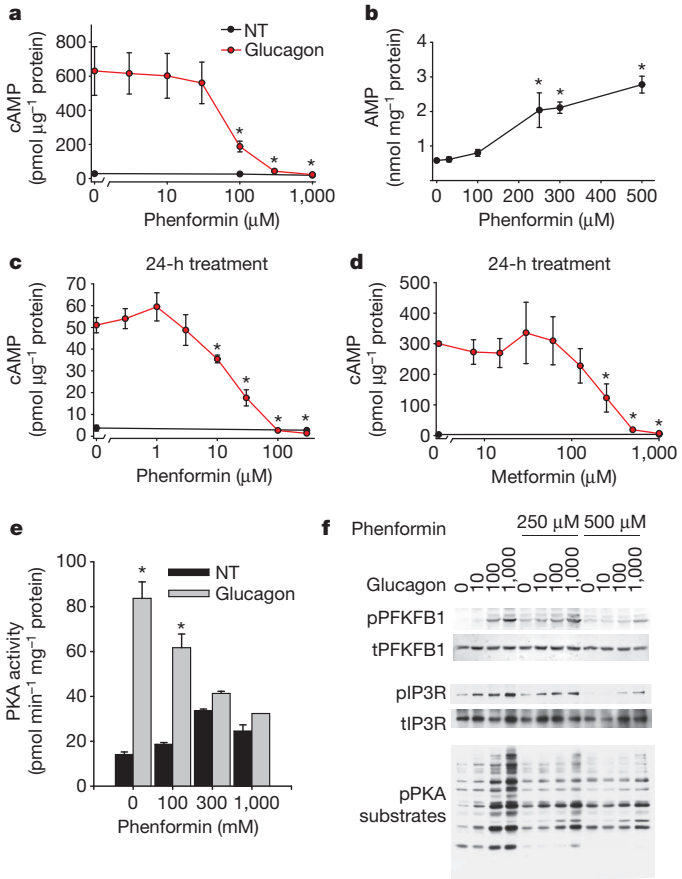

Figure 1 | Biguanides inhibit cAMP accumulation. **a**, Primary hepatocytes were incubated with the indicated phenformin concentrations for 2 h, 5 nM glucagon or no treatment (NT) for 15 min, lysed, and assayed for total cellular cAMP and protein. $N = 4$ for each point. **b**, Primary hepatocytes incubated with the indicated concentration of phenformin for 2 h were extracted with perchloric acid and cellular nucleotides quantified by high-performance liquid chromatography (HPLC). $N = 4$ for each point. **c**, **d**, Primary hepatocytes were incubated with the indicated concentration of phenformin (**c**) or metformin (**d**) for 24 h, treated with 5 nM glucagon, lysed, and assayed for total cellular cAMP. $N = 4$ for each point. **e**, Primary hepatocytes were incubated with the indicated concentrations of phenformin for 2 h, treated with 5 nM glucagon, lysed, and PKA kinase activity determined. $N = 6$ for 0 and 1,000 µM phenformin groups, $N = 4$ for 100 and 300 µM phenformin groups. **f**, Primary hepatocytes were incubated with phenformin for 2 h, then with glucagon, and protein was analysed by western blot with the phospho- (p)PKA substrate motif antibody, total (t) and phospho- (p)PFKFB1 antibodies, and total and phospho-IP3R antibodies. Error bars represent standard error of the mean (s.e.m.).

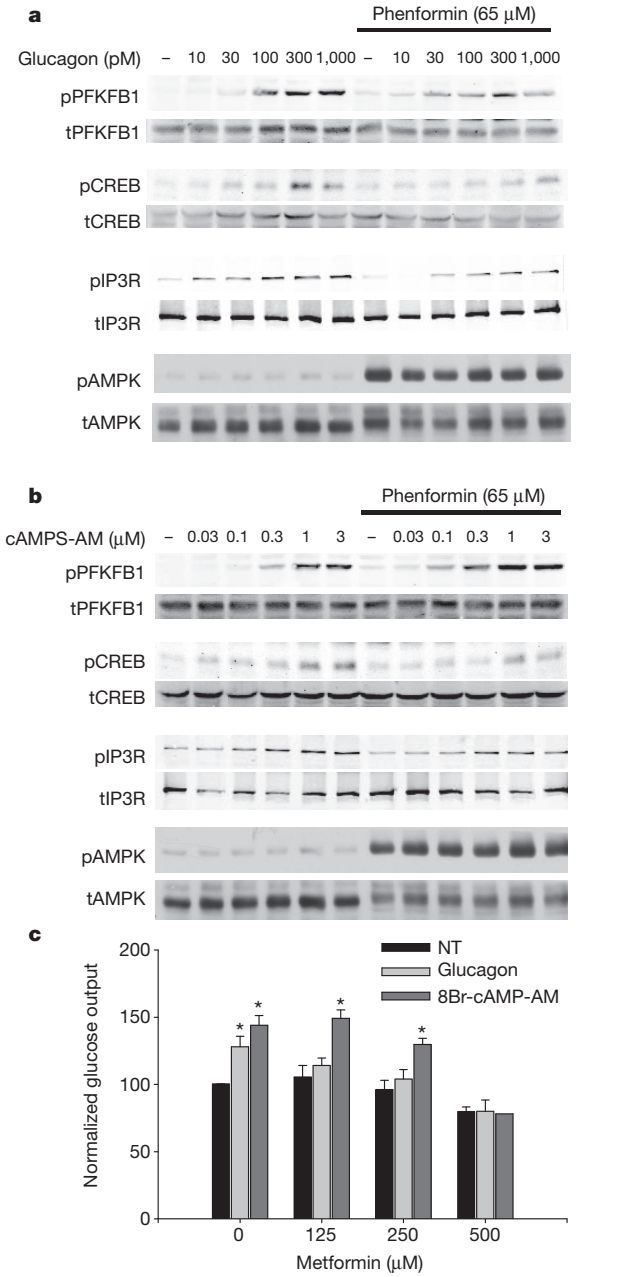

Figure 2 | Biguanides inhibit glucagon signalling. **a**, **b**, Primary hepatocytes were cultured for 18 h in the presence or absence of 65 µM phenformin and for 15 min with the indicated concentrations of glucagon (**a**) or the cell-permeable PKA agonist SP-8Br-cAMPS-AM (**b**). Western blot analysis of total (t) and phosphorylated (p) PFKFB1, CREB, IP3R and AMPK. **c**, Cells were treated with the indicated concentration of metformin and either 1 nM glucagon or 3 µM SP-8Br-cAMPS-AM, or were left untreated (NT), for 14 h and then glucose output measured for 5 h. Data represent the means of three experiments, $N = 6$ for each experiment. Error bars represent s.e.m.

of PKA. Both glucagon and SP-8Br-cAMPS-AM increased glucose output from primary hepatocytes; however, treatment of hepatocytes with therapeutic concentrations of metformin prevented glucagon- but not SP-8Br-cAMPS-AM-stimulated increases in glucose output (Fig. 2b). Of note, higher concentrations of metformin reduced basal as well as glucagon- and SP-8Br-cAMPS-AM-dependent glucose output. If the major actions of biguanide were mediated by decreases in cAMP, one would expect the drug to be ineffective in cells in which PKA has already been inhibited. In hepatocytes overexpressing a dominant-negative PKA regulatory subunit that is unable to bind cAMP, PKA activity was necessary for glucagon stimulation of glucose output, and biguanides did not reduce the rate of glucose output any further (Supplementary Fig. 6c).

As the biguanides and other drugs we used activated AMPK in parallel to the reduction in cAMP, we asked whether the kinase was required for the effects of biguanides. Mice homozygous for the floxed alleles of both catalytic α1 and α2 subunits of the AMPK complex were infected with adeno-associated virus expressing Cre recombinase, and western blots confirmed deletion of AMPK α protein and loss of phenformin-dependent phosphorylation of the AMPK substrate acetyl-CoA carboxylase (ACC) (Fig. 3a). In hepatocytes lacking any detectable AMPK activity, phenformin blocked glucagon-dependent cAMP accumulation in a manner indistinguishable from that in control cells (Fig. 3b). AICAR also reduced cAMP in the absence of AMPK (Supplementary Fig. 4b). These data show that the effects of biguanides on cAMP metabolism are independent of AMPK.

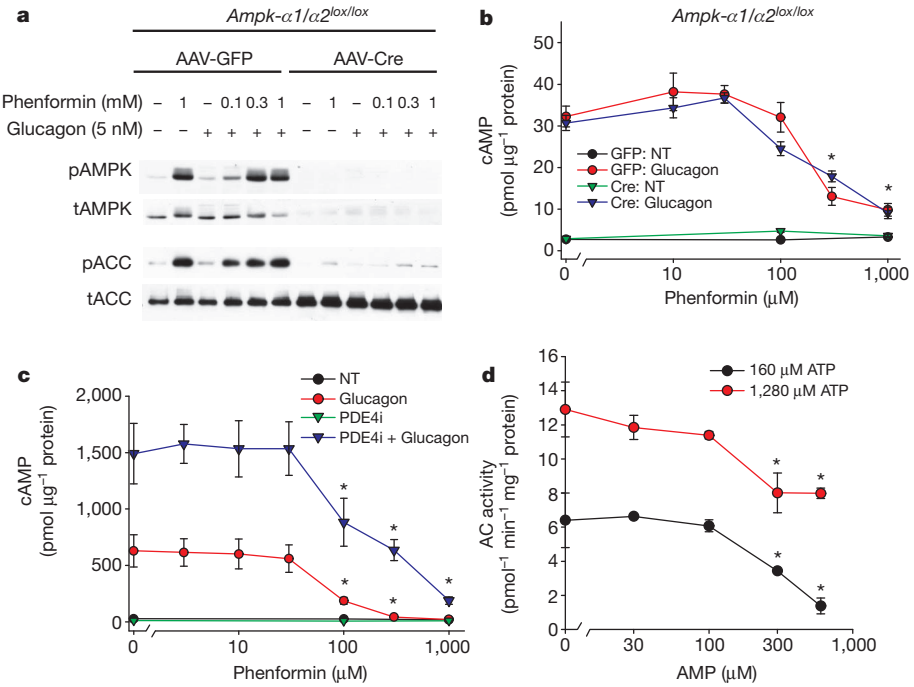

Figure 3 | Mechanism of biguanide effect on cAMP production. **a**, *Ampk-α1/α2*$^{lox/lox}$ mice were infected with AAV-TBG-GFP or AAV-TBG-Cre virus and 14 days later primary hepatocytes were isolated. Cells were treated with the indicated concentrations of phenformin for 2 h followed by 5 nM glucagon or no treatment (NT) for 15 min. **a**, Total cellular protein was analysed by western blot for total (t) and phosphorylated (p) T172 AMPK and total and phospho-S79 ACC. **b**, Hepatocytes were lysed and total cellular cAMP levels were quantified by ELISA. $N = 4$ for all points. **c**, Primary hepatocytes were incubated with the indicated concentrations of phenformin for 2 h and 50 µM RO-20-1724 (PDE4 inhibitor; PDE4i) for the final 30 min. Cells were then treated with 5 nM glucagon for 15 min, lysed, and total cellular cAMP was assayed. $N = 4$ for all points. **d**, The membrane fraction of primary hepatocytes was isolated by differential centrifugation and used in assays for adenylyl cyclase activity in the presence of the indicated AMP and ATP concentrations, 100 nM glucagon and 100 µM GTP. $N = 6$ for all points. Error bars represent s.e.m.

To determine whether reduction of the glucagon-dependent increase in cAMP was caused by activation of cAMP phosphodiesterase (PDE), we used pharmacological inhibitors of PDEs. If inhibition of cAMP degradation did not also block the effect of phenformin on cAMP, it would imply that the site of action was unlikely to be PDE. Exposure of glucagon-treated hepatocytes to 3-isobutyl-1-methylxanthine (IBMX; a non-specific PDE inhibitor) or Ro-20-1724 (a specific PDE4 class inhibitor), but not cilostamide (a specific PDE3 class inhibitor), increased cAMP levels, indicating that PDE4 is the major cAMP-degrading enzyme in these cells (Supplementary Fig. 7a). Even in the presence of IBMX or Ro-20-1724, phenformin inhibited glucagon-stimulated accumulation of cAMP (Supplementary Fig. 7a). Moreover, Ro-20-1724 did not affect the dose responsiveness of hepatocytes to phenformin (Fig. 3c). To resolve phenformin's site of action further, we measured its effects on cAMP accumulation in response to forskolin, which binds to and stimulates adenylyl cyclase independent of the activated Gα protein. Both phenformin and AICAR blocked cAMP accumulation by both glucagon and forskolin to the same extent, indicating that the effects of these drugs were unlikely to be due to modulation of the glucagon receptor or G-protein signalling (Supplementary Figs 4c and 7b).

As phenformin blocked glucagon-induced cAMP production at concentrations that correlated well with its effect on AMP levels, we sought to determine whether AMP could directly inhibit adenylyl cyclase, as has been reported previously[17–20]. Forskolin and glucagon stimulated adenylyl cyclase activity about fourfold in membranes isolated from primary mouse hepatocytes (Supplementary Fig. 8a). AMP inhibited glucagon-stimulated adenylyl cyclase activity when ATP was present at 160 µM, which represents typical conditions for the assay, as well as at the more physiological concentration of 1.28 mM ATP (Fig. 3d). To determine whether AMP accumulated in the livers of metformin-treated mice to levels sufficient to inhibit adenylyl cyclase, we measured hepatic AMP in fasted wild-type mice. Consistent with a recent report, we found the concentration of AMP to be 2.3 mM and to rise to 2.9 mM after treatment with metformin in mice fed a normal chow diet[21,22] (Supplementary Table 1). Because these values seemed unphysiologically high, we also measured nucleotides in primary hepatocytes (Supplementary Table 2). In untreated cells, the AMP concentration was 215 µM, which correlated well with a value of 300 µM reported previously[23] in perfused rat liver using ^{31}P NMR. The AMP concentration in hepatocytes rose to over 1 mM in a dose-dependent manner upon treatment with phenformin (Supplementary Table 2).

To test whether the effects of biguanides on the accumulation of cAMP in primary hepatocytes were representative of its actions *in vivo*, we examined the effects of metformin after injection of glucagon into mice. Glucagon rapidly increased blood glucose, an effect that was blunted by pre-administration of metformin (Fig. 4a). Gavage of mice with metformin increased both AMPK and ACC phosphorylation, indicating a decrease in the cellular energy charge of the liver (Supplementary Fig. 9a). Most importantly, metformin abrogated the subsequent glucagon-dependent increase in hepatic cAMP, PKA activity and phosphorylation of PKA substrates, demonstrating *in vivo* blockade of this pathway by biguanides (Fig. 4b, c). To assess the effect of metformin on the action of endogenous glucagon, fasted mice were given an oral gavage of water or 250 mg kg^{-1} metformin, and 1 h later their blood glucose levels were determined and hepatic tissue was collected. This dose of metformin caused a significant drop in the blood glucose levels and an elevation in hepatic AMP (Supplementary Fig. 9b and Supplementary Table 1), which correlated well with a concomitant reduction in hepatic cAMP content (Fig. 4d–f). We next tested the effects of metformin in diabetic mice fed a high-fat diet (HFD) for 10 weeks. These mice had elevated fasting glucose levels and hepatic AMP compared to chow-fed animals (Supplementary

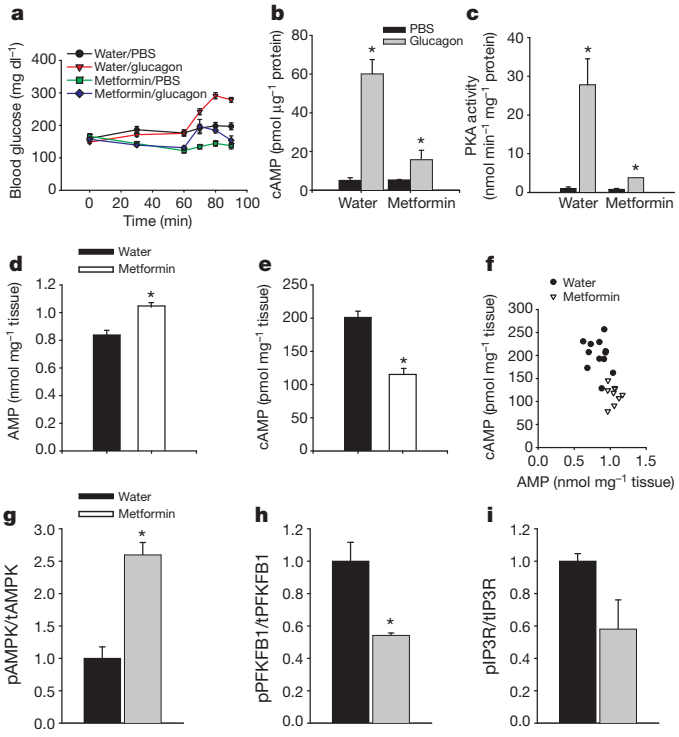

Figure 4 | Biguanides antagonize glucagon signalling *in vivo*. **a**, Mice were gavaged with 500 mg kg^{-1} metformin and 1 h later were injected intraperitoneally with 200 μg kg^{-1} glucagon, and glucose levels were measured at the indicated times. $N = 6$ for water/PBS and metformin/glucagon, $N = 7$ for water/glucagon and metformin/PBS. **b**, **c**, Fed mice were fasted for 1 h and gavaged with water or 500 mg kg^{-1} body weight of metformin. One-hour later mice were injected intraperitoneally with 2 mg kg^{-1} glucagon, and liver tissue was collected 5 min later. Liver was analysed for total hepatic cAMP by ELISA (**b**; $N = 3$ for each group) and total hepatic PKA activity (**c**; $N = 7, 8, 6$ and 7 for water/PBS, water/glucagon, metformin/PBS and metformin/glucagon, respectively). *$P < 0.05$ compared to PBS. **d**–**f**, 18-h fasted mice were gavaged with water or 250 mg kg^{-1} metformin, 1 h later liver tissue was collected, hepatic metabolites were extracted with perchloric acid and total hepatic AMP (**d**) and cAMP (**e**) levels were assayed. $N = 12$ and 9 for the water and metformin groups, respectively. **g**–**i**, Mice fed HFD for 10 weeks were fasted overnight, gavaged with either water or 250 mg kg^{-1} metformin, and after 1 h liver tissue was collected for western blot analysis of the phosphorylation status of AMPK (**g**), PFKFB1 (**h**) and IP3R (**i**). $N = 3$ for each group. Error bars represent s.e.m.

Table 1 and Supplementary Fig. 10a, b). Fasted HFD mice were given an oral gavage of water or 250 mg kg^{-1} metformin and 1 h later blood glucose was determined and hepatic tissue collected. Metformin significantly lowered blood glucose levels and elevated hepatic AMP (Supplementary Fig. 10c and Supplementary Table 1). Importantly, treatment of these mice with metformin led to a reduction in the phosphorylation of two key PKA target proteins, PFKFB1 and the IP3R, and increased AMPK phosphorylation (Fig. 4g–i and Supplementary Fig. 10d). The lack of change in Akt phosphorylation indicated that metformin was not affecting insulin responsiveness acutely (Supplementary Fig. 10d, e).

Understanding the mechanism by which the drug metformin reduces hepatic glucose output is of considerable importance. Using a variety of biochemical and cell biological methods, we have confirmed earlier reports of an effect of biguanides on cAMP[24–27]. Furthermore, we have shown that it is through an elevation in intracellular AMP that metformin substantially abrogates the activation of adenylyl cyclase by glucagon. This results in a reduction in the phosphorylation of key substrates for maintaining hepatic glucose output. For nearly 40 years it has been recognized that molecules containing an adenine moiety bind to the 'P site' of adenylyl cyclase and inhibit its activity[17]. Although the endogenous P-site ligand has been suggested to be AMP, the physiological or pharmacological relevance of this regulatory event has not previously been recognized[17–20,28]. We now provide support for the idea that therapeutic levels of metformin induce a mild energetic stress in hepatocytes, resulting in an increase in AMP concentration to levels capable of directly inhibiting adenylyl cyclase. These studies suggest that the P site of adenylate cyclase might represent a novel target for the development of therapeutics for the treatment of insulin resistance and type-2 diabetes.

METHODS SUMMARY

Primary hepatocytes were isolated by collagenase perfusion as described previously[29]. Adenine nucleotides were extracted from cells and liver with perchloric acid and measured by ion-pair reversed-phase (RP)-HPLC. cAMP in primary hepatocytes and frozen liver tissue was measured by ELISA (GE Healthcare) using the manufacturer's lysis buffer. PKA activity was assayed in cell lysates as PKI-sensitive Kemptide phosphorylation. PKA FRET-activity probes were used to examine intracellular PKA activity on a spinning-disc confocal microscope[16]. Adenylyl cyclase assays were performed using adenosine-5′-triphosphate [α-^{32}P] (American Radiolabelled Chemicals), and cAMP was quantified as previously described[30]. Glucose output studies in primary hepatocytes from fasted mice were carried out in Krebs buffer containing gluconeogenic substrates (20 mM lactate, 2 mM pyruvate, 10 mM glutamine) and were quantified using hexokinase-based glucose assays (Sigma). For *in vivo* experiments, metformin was gavaged at the indicated dosage and glucagon was injected intraperitoneally at the indicated dosages. Tissues were collected rapidly from anaesthetized mice and frozen in pre-cooled metal clamps. All results are expressed as the mean ± s.e.m. All two-group comparisons were deemed statistically significant by unpaired two-tailed Student's *t*-test if $P < 0.05$.

Full Methods and any associated references are available in the online version of the paper.

Received 25 January; accepted 22 November 2012.
Published online 6 January 2013.

1. DeFronzo, R. A., Simonson, D. & Ferrannini, E. Hepatic and peripheral insulin resistance: a common feature of type 2 (non-insulin-dependent) and type 1 (insulin-dependent) diabetes mellitus. *Diabetologia* **23,** 313–319 (1982).
2. Postic, C., Dentin, R. & Girard, J. Role of the liver in the control of carbohydrate and lipid homeostasis. *Diabetes Metab.* **30,** 398–408 (2004).
3. Nathan, D. M. *et al.* Medical management of hyperglycemia in type 2 diabetes: a consensus algorithm for the initiation and adjustment of therapy: a consensus statement of the American Diabetes Association and the European Association for the Study of Diabetes. *Diabetes Care* **32,** 193–203 (2009).
4. Foretz, M. *et al.* Metformin inhibits hepatic gluconeogenesis in mice independently of the LKB1/AMPK pathway via a decrease in hepatic energy state. *J. Clin. Invest.* **120,** 2355–2369 (2010).
5. Inzucchi, S. E. *et al.* Efficacy and metabolic effects of metformin and troglitazone in type II diabetes mellitus. *N. Engl. J. Med.* **338,** 867–873 (1998).
6. Goodarzi, M. O. & Bryer-Ash, M. Metformin revisited: re-evaluation of its properties and role in the pharmacopoeia of modern antidiabetic agents. *Diabetes Obes. Metab.* **7,** 654–665 (2005).
7. El-Mir, M. Y. *et al.* Dimethylbiguanide inhibits cell respiration via an indirect effect targeted on the respiratory chain complex I. *J. Biol. Chem.* **275,** 223–228 (2000).
8. Owen, M. R., Doran, E. & Halestrap, A. P. Evidence that metformin exerts its anti-diabetic effects through inhibition of complex 1 of the mitochondrial respiratory chain. *Biochem. J.* **348,** 607–614 (2000).
9. Shaw, R. J. *et al.* The kinase LKB1 mediates glucose homeostasis in liver and therapeutic effects of metformin. *Science* **310,** 1642–1646 (2005).
10. Zhou, G. *et al.* Role of AMP-activated protein kinase in mechanism of metformin action. *J. Clin. Invest.* **108,** 1167–1174 (2001).
11. D'Alessio, D. The role of dysregulated glucagon secretion in type 2 diabetes. *Diabetes Obes. Metab.* **13** (suppl. 1), 126–132 (2011).
12. Jiang, G. & Zhang, B. B. Glucagon and regulation of glucose metabolism. *Am. J. Physiol. Endocrinol. Metab.* **284,** E671–E678 (2003).
13. Unger, R. H. & Cherrington, A. D. Glucagonocentric restructuring of diabetes: a pathophysiologic and therapeutic makeover. *J. Clin. Invest.* **122,** 4–12 (2012).
14. Tucker, G. T. *et al.* Metformin kinetics in healthy subjects and in patients with diabetes mellitus. *Br. J. Clin. Pharmacol.* **12,** 235–246 (1981).
15. Wilcock, C. & Bailey, C. J. Accumulation of metformin by tissues of the normal and diabetic mouse. *Xenobiotica* **24,** 49–57 (1994).
16. Allen, M. D. & Zhang, J. Subcellular dynamics of protein kinase A activity visualized by FRET-based reporters. *Biochem. Biophys. Res. Commun.* **348,** 716–721 (2006).
17. Fain, J. N., Pointer, R. H. & Ward, W. F. Effects of adenosine nucleosides on adenylate cyclase, phosphodiesterase, cyclic adenosine monophosphate accumulation, and lipolysis in fat cells. *J. Biol. Chem.* **247,** 6866–6872 (1972).

18. Blume, A. J. & Foster, C. J. Mouse neuroblastoma adenylate cyclase. Adenosine and adenosine analogues as potent effectors of adenylate cyclase activity. *J. Biol. Chem.* **250,** 5003–5008 (1975).
19. Londos, C. & Preston, M. S. Regulation by glucagon and divalent cations of inhibition of hepatic adenylate cyclase by adenosine. *J. Biol. Chem.* **252,** 5951–5956 (1977).
20. Johnson, R. A., Yeung, S. M., Stubner, D., Bushfield, M. & Shoshani, I. Cation and structural requirements for P site-mediated inhibition of adenylate cyclase. *Mol. Pharmacol.* **35,** 681–688 (1989).
21. Berglund, E. D. *et al.* Hepatic energy state is regulated by glucagon receptor signaling in mice. *J. Clin. Invest.* **119,** 2412–2422 (2009).
22. Stoll, B., Gerok, W., Lang, F. & Haussinger, D. Liver cell volume and protein synthesis. *Biochem. J.* **287,** 217–222 (1992).
23. Masson, S. & Quistorff, B. The ^{31}P NMR visibility of ATP in perfused rat liver remains about 90%, unaffected by changes of metabolic state. *Biochemistry* **31,** 7488–7493 (1992).
24. Gawler, D. J., Wilson, A. & Houslay, M. D. Metformin treatment of lean and obese Zucker rats modulates the ability of glucagon and insulin to regulate hepatocyte adenylate cyclase activity. *J. Endocrinol.* **122,** 207–212 (1989).
25. Torres, T. P. *et al.* Impact of a glycogen phosphorylase inhibitor and metformin on basal and glucagon-stimulated hepatic glucose flux in conscious dogs. *J. Pharmacol. Exp. Ther.* **337,** 610–620 (2011).
26. Yu, B., Pugazhenthi, S. & Khandelwal, R. L. Effects of metformin on glucose and glucagon regulated gluconeogenesis in cultured normal and diabetic hepatocytes. *Biochem. Pharmacol.* **48,** 949–954 (1994).
27. Zhang, T. *et al.* Mechanisms of metformin inhibiting lipolytic response to isoproterenol in primary rat adipocytes. *J. Mol. Endocrinol.* **42,** 57–66 (2009).
28. Fain, J. N. & Malbon, C. C. Regulation of adenylate cyclase by adenosine. *Mol. Cell. Biochem.* **25,** 143–169 (1979).
29. Miller, R. A. *et al.* Adiponectin suppresses gluconeogenic gene expression in mouse hepatocytes independent of LKB1-AMPK signaling. *J. Clin. Invest.* **121,** 2518–2528 (2011).
30. Post, S. R., Ostrom, R. S. & Insel, P. A. Biochemical methods for detection and measurement of cyclic AMP and adenylyl cyclase activity. *Methods Mol. Biol.* **126,** 363–374 (2000).

Supplementary Information is available in the online version of the paper.

Acknowledgements This work was supported by National Institutes of Health (NIH) grants RO1 DK56886 and PO1 DK49210 (M.J.B.) and F32 DK079572 (R.A.M.), the Association pour l'Etude des Diabètes et des Maladies Métaboliques (ALFEDIAM) (to M.F.), the Programme National de Recherche sur le Diabète (PNRD) (to M.F. and B.V.) and the Institut Benjamin Delessert (to M.F.). Microscopy was performed in the University of Pennsylvania Cell and Developmental Biology Microscopy Core Facility. The Transgenic/Knockout, Mouse Phenotyping, Viral Vector and Biomarker Cores of the University of Pennsylvania Diabetes and Endocrinology Research Center (NIH grant P30 DK19525) were instrumental in this work.

Author Contributions R.A.M. and Q.C. performed experiments; R.A.M. and M.J.B. designed experiments and wrote the manuscript. J.X. generated the phospho-S33 PFKFB1 antibody. M.F. and B.V. generated the AMPK α1 and α2 floxed alleles. J.X., M.F. and B.V. critically read the manuscript.

Author Information Reprints and permissions information is available at www.nature.com/reprints. The authors declare no competing financial interests. Readers are welcome to comment on the online version of the paper. Correspondence and requests for materials should be addressed to M.J.B. (birnbaum@mail.med.upenn.edu).

METHODS

Reagents and materials. Reconstituted GlucaGen (Novo Nordisk) was used for all glucagon studies. Phosphorylase kinase B antibody was purchased from Acris Antibodies. Total PFKFB1 antibody was purchased from Santa Cruz Biotechnology. The rabbit anti-PFKFB1 phospho-S33 antibody was produced by Cell Signaling Technology. All other antibodies were purchased from Cell Signaling Technology. The SP-8br-cAMPS-AM was purchased from AXXORA, LLC. All additional reagents were purchased from Sigma Aldrich. Adeno-associated virus expressing the PKA dominant-negative Rab mutant of the PKA RIα subunit from a liver-specific TBG promoter was produced and purified in the University of Pennsylvania Viral Vector Core.

Mice. Mice were housed in a facility on a 12-h light–dark cycle with free access to food and water. All procedures were reviewed and approved by the Institutional Animal Care and Use Committee at the University of Pennsylvania. Blood glucose values were measured with OneTouch Ultra glucose analyser. Mice were killed either by rapid cervical dislocation or, for studies examining nucleotide levels, by anaesthetization with 2,2,2-tribromoethanol. Liver samples were rapidly removed and frozen in pre-cooled metal tongs and frozen in liquid nitrogen. The time from liver ischaemia to frozen tissue was approximately 30 s and 5 s for cervical dislocation or anaesthetic-based methods, respectively.

Primary hepatocytes. Primary hepatocytes were isolated from mice with a modified two-step perfusion method using Liver Perfusion Media and Liver Digest Buffer (Invitrogen). Cells were plated in collagen-I-coated 6- or 12-well plates (at 2 or 1 million cells per well, respectively) in M199 media plus 10% FBS plus penicillin/streptomycin plus 1 nM insulin/100 nM T3/100 nM dexamethasone. After 3 h of attachment, the media was replaced with fresh media and the cells were incubated in culture overnight. Experiments were performed 18–24 h after isolation of the cells. For 24-h treatments of hepatocytes, compounds were added after the 3-h attachment period.

Quantification of adenine nucleotides. Adenine nucleotides were extracted from primary hepatocytes as described previously[29]. For quantification of liver nucleotides, samples were harvested from anaesthetized mice and immediately frozen. Approximately 50-mg pieces of liver were weighed and nucleotides were extracted with 0.5 M perchloric acid. The insoluble materials were pelleted by centrifugation and the soluble fraction was neutralized with 0.25 volumes 2 M KOH, 1 M PO_4 pH 7.8. Neutralized samples were stored at −80 °C. Perchloric-acid-soluble materials were separated by isocratic elution in an ion-pair reverse-phase (RP)-HPLC system (the buffer used was 200 mM KH_2PO_4 pH 6.25, 5 mM tetrabutylammoniumphosphate (TBAP), 3% acetonitrile). AMP, ADP and ATP peak areas were calculated and converted to molar amounts through comparison to standard curves generated from quantification of known quantities of pure nucleotides separated under identical conditions. Values of nmol mg^{-1} protein were converted to concentrations using the cell volume of primary hepatocytes[22].

cAMP quantification. cAMP was assayed using a cAMP ELISA kit (GE Healthcare) according to the manufacturer's alternative lysis protocol. For primary hepatocytes, cells in 12-well plates were lysed with 250 µl of lysis buffer 1B and cAMP quantified. For liver samples, cAMP was measured by ELISA, and normalized to total liver weight.

***In vitro* PKA assays.** Total soluble lysates from either primary hepatocytes or liver were obtained using lysis buffer (1% Triton X-100, 150 mM NaCl, 20 mM PO_4 pH 7.4). PKA activity was assayed using ATP-γ-^{32}P using a PKA Kinase Assay Kit (Millipore) as Kemptide phosphorylation that was sensitive to PKI inhibition.

Microscopy. Primary hepatocytes were plated on coverslip bottom tissue culture plates coated with collagen I and infected with adenovirus expressing the PKA FRET reporter AKAR3 (ref. 16). Eighteen hours after infection the media was changed to imaging media (M199 media lacking sodium bicarbonate and phenol red supplemented with 20 mM HEPES pH 7.4) and cells were studied using a Zeiss confocal microscope. FRET (442 nm excitation/560 nm emission), CFP (442 nm excitation/480 nm emission) and YFP (523 nm excitation/560 nm emission) channel images of hepatocytes were acquired at 20 s intervals. 5 nM glucagon was added as 500 µl of 50 nM glucagon in pre-warmed imaging buffer to 2 ml of media. The FRET ratio ((FRET background)/(CFP background)) was taken from a random segment of the cytoplasm and nucleus, with one region of interest per cell, and over 40 regions of interest contributing to each condition. Ratios were normalized to the first 4 min of acquisition time.

Glucose output assays. Primary hepatocytes were isolated from 12-h fasted mice and plated in M199 media with 10% FBS for 4 h. After attachment the media was replaced with serum-free M199 media with 100 nM dexamethasone and 100 nM T3, as well as the indicated drugs. After 14 h the cells were washed with glucose output media (118 mM NaCl, 4.7 mM KCl, 1.2 mM $MgSO_4$, 1.2 mM KH_2PO_4, 1.2 mM $CaCl_2$, 20 mM $NaCO_3$, 25 mM HEPES pH 7.4 and 0.025% BSA), and glucose output was measured in fresh glucose output media supplemented with gluconeogenic substrates (20 mM lactate, 2 mM pyruvate, 10 mM glutamine) for 5 h. Glucose output was normalized to total protein and expressed as the per cent of untreated basal glucose output.

Adenylyl cyclase assays. Adenylyl cyclase activity was measured as previously described[30]. Membrane preparations were obtained from primary hepatocytes in 15-cm plates. Cells were washed with PBS and lysed with hypotonic buffer (10 mM Tris pH 7.4, 5 mM EDTA) and 10 strokes of a dounce homogenizer. Unlysed cells and nuclei were pelleted and removed by centrifugation at 3,000*g*. The supernatant was centrifuged at 12,000*g* to pellet membranes, which were resuspended in lysis buffer and frozen at −80 °C. Adenylyl cyclase assays were performed under various ATP concentrations with tracer quantities of adenosine-5′-triphosphate [α-^{32}P] (American Radiolabelled Chemicals) with the following final assay conditions: 15 mM HEPES pH 7.4, 200 mM NaCl, 1 mM EGTA, 10 mM $MgCl_2$, 1 mM IBMX, 10 mM phosphocreatine, 60 U ml^{-1} creatine kinase (Sigma Aldrich). Assays were performed at 30 °C for 10 min and stopped with the addition of an equal volume of stop solution (2% SDS, 1 mM ATP, 1 mM cAMP, ~2,000 c.p.m. [^{3}H]cAMP (refs 2, 8) (American Radiolabelled Chemicals)). Eight-hundred millilitres of water was added and this solution was purified by chromatography using Dowex 50WX8-200 (Sigma Aldrich) and Neutral Alumina (Sigma Aldrich) columns. The cAMP produced was measured as [^{32}P]cAMP, recovered, and was corrected for recovery by calculating recovery of [^{3}H]cAMP (refs 2, 8). The specific activity of ATP (c.p.m./total ATP) was determined before and after incubation with purified hepatocyte membrane fractions and adenylyl cyclase assay buffer in the presence and absence of AMP. No significant reduction in specific activity or total ATP was observed (Supplementary Fig. 8b, c).

Statistical analysis. All results are expressed as the mean ± s.e.m. All two-group comparisons were deemed statistically significant by unpaired two-tailed Student's *t*-test if $P < 0.05$. All *in vitro* studies are either compilations of three independent experiments or representative of three independent experiments. The number of mice used in each *in vivo* condition is indicated in the figure legends.